Eletrônica de Potência
Open Journal of Power Electronics

Received July 17, 2024; accepted September 03, 2024; Date of publication September 09, 2024.
The review of this paper was arranged by Associate Editor Roberto F. Coelho and Editor-in-Chief Heverton A. Pereira.

*Digital Object Identifier http://doi.org/10.18618/REP.e202432*

# VFD-based Coordinated Centralized/decentralized Control to Support Offshore Electrical Power Systems with Wind Power Penetration

**João Marcus Soares Callegari**[1], **Danilo Iglesias Brandao**[1]

[1]Universidade Federal de Minas Gerais, Graduate Program in Electrical Engineering, Belo Horizonte, MG, Brazil.

e-mail: jmscallegari@ufmg.br; dibrandao@ufmg.br

**ABSTRACT** This paper proposes a coordinated centralized/decentralized control designed to concomitantly manage the power factor and mitigate voltage variations at the main feeder of an oil and gas offshore platform. The centralized action (i.e., power factor control) is decoupled from the decentralized one (i.e., voltage support) due to the significant disparity in dynamics of the commands sent to the active front-end variable frequency drives (AFE-VFDs). The AFE-VFDs are embedded with a proposed V-Q inverse droop curve, while being remotely coordinated by a central controller using a low-bandwidth communication link. Unlike other strategies, the proposed control is effective in handling unplanned events and unpredictable disturbances. Simulations are conducted to compare the proposed strategy with a literature solution considering a typical Brazilian floating production storage and offloading platform, from Mero Oil Field.

**KEYWORDS** Coordinated control; floating, production, storage, and offloading; power factor; variable frequency drives; voltage support.

## I. INTRODUCTION

Increasing power generation while reducing carbon emissions in floating production storage and offloading (FPSO) units is challenging. The limited space and weight capacity on FPSOs make adding new equipment difficult. The integration of floating offshore wind power to FPSO platforms stands out as a promising solution for both of these challenges [1]. However, wind speed fluctuations and the inherent weakness of FPSO power systems can cause voltage and frequency variations [2]. Exploiting new functionalities of already used equipment in FPSO, as variable frequency drives (VFDs), is quite appealing to mitigate those issues.

Conventional VFDs use a diode front-end input, which is cost-effective and widely used [3]. However, the passive rectifier stage draws high levels of harmonic currents, which is undesirable in offshore systems. This issue is overcome by employing active front-end VFDs (AFE-VFDs), in which the input waveform is less harmonic polluted and provides the capability of exchanging reactive power with the FPSO system [4]. To better exploit the use of these power electronics-based equipment, this paper proposes using the AFE-VFDs already installed at the FPSO to concomitantly regulate the power factor (PF) at the synchronous generator (SG) terminals and support voltage variation of unplanned events and unpredictable disturbances, like direct on-line (DOL) motor starting, intermittence of wind power and grid faults.

There are very few papers addressing coordinated centralized/decentralized control in offshore platforms. Reference [5] shows the worsening effect on power quality metrics in a Brazilian FPSO power system due to the high penetration of wind-based power generation. Reference [6] shows the mitigation of distortion, unbalance, and reactive power terms by leveraging the power availability of distributed AFE-VFDs in a Brazilian FPSO. In [7], peak shaving and spinning reserve support are achieved using a battery energy storage system for an FPSO at the North Sea. The authors of [8] proposed a purely decentralized control embedded into AFE-VFDs to mitigate voltage fluctuations on oil and gas platforms caused by connecting wind power systems through short- and long-umbilical cables. Medeiros *et al.* [9] proposed a decentralized frequency-voltage-var control embedded in AFE-VFDs to provide frequency and voltage support in a typical FPSO unit with wind power integration.

By incorporating a central controller (CC), a superior level of control is provided, enabling the management of the PF of the SGs and enhancing both the efficiency and electrical flexibility of the FPSO. None of the previously mentioned strategies offer the simultaneous benefits of fast decentralized voltage support and slower centralized PF control, which is a highly desired feature. To the best of the author's knowledge, only [10] exploits the embedded VFD power electronics steered by a CC to achieve coordinated PF of SGs in steady-state and to provide voltage support through the AFE-VFD embedded volt-var curve during DOL motor start. However, this voltage support is only available during planned events signaled by the FPSO operator.

In contrast to [10], the proposed coordinated control provides both steady-state and transient FPSO voltage support during unplanned events and unpredictable disturbances, while keeping the PF regulated. The FPSO electrical power system is simulated in MATLAB/Simulink®. Guidelines for proper tuning of the proposed strategy parameters are also provided. Conclusions are drawn based on the performance improvements of the proposed strategy during both steady-state conditions (e.g., intermittent wind power) and transient-state conditions (e.g., planned/unplanned DOL starts, generator outages, and faults).

## II. POWER SYSTEM AND PROPOSED CONTROL

Fig. 1 shows the schematic of the electrical power system of a typical Brazilian FPSO from Mero Oil Field. It comprises three main gas-driven synchronous generators (SGs). The bar nomenclature, XYn, is as follows: X represents the top (T) or bottom (B) bar, Y indicates the left (L) or right (R) bar, and $n$ is the number of the bar-connected equipment. Circuit breakers CB1, CB2, and CB3 are closed, forming a radial grid. The FPSO electrical system supplies equivalent low-voltage (LV) loads interfaced through step-down transformers, forty-six squirrel-type double-cage induction motors, and medium voltage (MV) loads. The loads on bars TLn, TRn, BLn, and BRn represent motor groups as detailed in [4]. Power ratings of the loads are shown in Fig.1, with more details in [10].

A 50 MW wind energy conversion system (WECS) connects to the FPSO via a 12 km subsea umbilical cable, where the energy is conveyed at 33 kV and subsequently reduced to 11 kV by an onboard FPSO step-down transformer. The integration of WECS, accounting for approximately 50% of the operating SG generation, increases energy availability for FPSO. However, due to the slow response of SG controllers, the intermittent nature of wind causes voltage and frequency fluctuations in the main feeder. In Fig. 1, the largest loads are 13 MW induction motors driving water injection pumps, controlled by two 16 MVA AFE-VFDs at TL4 and TR4 bars. A CC is placed on the FPSO main feeder, gathering and transmitting data packets, to achieve coordinated control targets by steering AFE-VFDs interfacing the largest motors. The proposed strategy can be applied to any FPSO with a CC installed at the location where PF regulation is desired, existing communication infrastructure, and AFE converters responsive to reactive power commands. The integration of WECS into the proposed strategy is possible, as long as the communication between CC and the WECS is robust and meets the latency requirements necessary for the centralized stable operation [11].

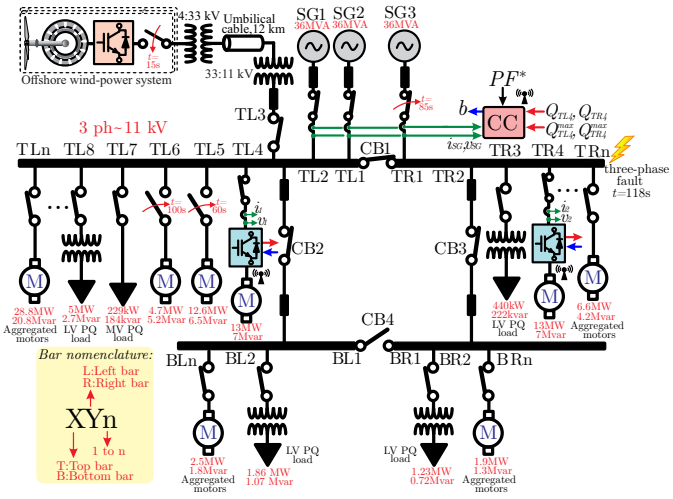


**FIGURE 1. Schematic of the offshore FPSO electrical power system.**

### A. Proposed coordinated centralized/decentralized control

Fig. 2(a) groups two control methods in a single block diagram. The switch in position ① selects the strategy addressed in [10], while position ② is the proposed method. The control ① regulates PF and supports planned voltage variation. Whereas the control ② enables PF regulation by means of remote control of AFE-VFDs by a CC, while autonomous voltage support is guaranteed by a decentralized V-Q inverse droop function. As highlighted by background color in Figure 2(a), the n-th AFE-VFD reactive power reference (i.e., $Q_n^*$) shows portions of centralized (i.e., $Q_n^{centr}$) and decentralized (i.e., $Q_n^{droop}$) commands:

$$Q_n^* = \overbrace{b \cdot Q_n^{max}}^{Centralized} - \overbrace{v_n^{rms} \cdot F(s) \cdot k}^{Decentralized}, \quad (1)$$

$$F(s) = \frac{s}{s+\omega_c}, \quad k = \frac{\Delta Q}{\Delta v} = \left( \frac{Q_n^{max} - Q_n^{min}}{v_{n,max}^{rms} - v_{n,min}^{rms}} \right), \quad (2)$$

where $b$ is the power scaling coefficient broadcast from CC to every AFE-VFDs, constrained to not overload these equipment [10]. $Q_n^{max}$ is the idle reactive power capacity available in n-th VFD with respect to its rated apparent power. $b$ is calculated periodically by CC similarly to [10], based on the actual status of AFE-VFDs to regulate PF. $v_n^{rms}$ is the AC RMS voltage measured at the point of connection of n-th AFE-VFD. $F$(s) is a high-pass filter with cutoff frequency of $\omega_c$ defined in (2), while $k$ is the V-Q inverse droop gain of the proposed strategy (unit var/V). From (2), $k$ can be tuned according to IEC 61892 voltage transient limits (i.e., within $v_{n,max}^{rms} = 1.2$ pu and $v_{n,min}^{rms} = 0.85$ pu), where $Q_n^{min} = -Q_n^{max}$. Centralized and decentralized controls operate simultaneously: centralized control manages long-term FPSO dynamics (based on communication response), while decentralized control handles short-term dynamics (based on VFD response time). Due to this response decoupling, transient voltage support and PF regulation is provided accordingly. Notably, the proposed strategy provides voltage support when $v_n^{rms}$ shows variations (i.e., $\Delta v \neq 0$). The voltage variation extraction is accomplished by $F$(s), where low-cutoff frequency slows the system response to eliminate the DC component from $v_{n,max}^{rms}$, and high-cutoff frequency filters out the fluctuation content of interest. $\Delta v$ is then multiplied by $k$ to generate the decentralized reference $Q^{droop}$. Figs. 2(b) and (c) show the effect of increasing $k$

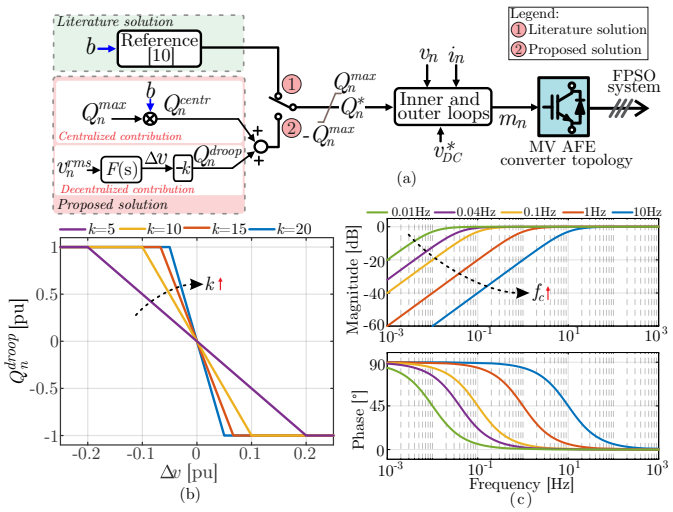


**FIGURE 2. (a) AFE-VFD control block diagram, incorporating both the proposed control strategy and the strategy from [10]. (b) $Q_n^{droop}$ behavior as a function of $k$. (c) Frequency response of the filter $F$(s) for different values of $f_c$.**

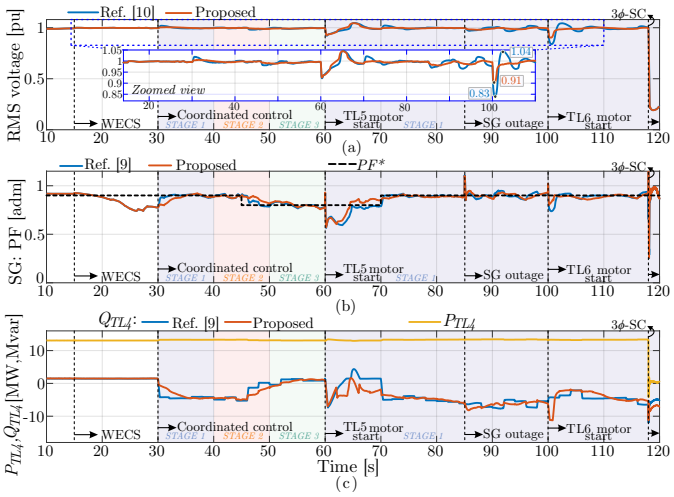


**FIGURE 3. Simulated results of coordinated control addressed in [10] and proposed coordinated control: (a) Main feeder RMS pu voltage. (b) PF at the SGs terminals. (c) VFD output active and reactive power terms.**

and $\omega_c = 2 \cdot \pi \cdot f_c$, respectively. The AFE-VFD reactive power response is more sensitive with increasing $k$, whereas increasing $\omega_c$ results in higher passband frequencies and faster filter response.

## III. SIMULATION RESULTS

For the sake of replicability, the electrical parameters of Fig. 1 can be found in [10]. Herein the proposed control is compared to [10], and then sensibility analysis is performed over $k$, $f_c$, and $t_{pbc}$ parameters. Also, $t_{pbc}$ is the centralized control communication time between CC and AFE-VFDs, which should be within the expected range for offshore systems [12].

### *A. Comparison of the proposed control strategy with the literature solution*

Fig. 3 shows the simulation results of FPSO under two operating scenarios: ($i$) coordinated centralized/decentralized multi-stage control addressed in [10]; and ($ii$) proposed coordinated centralized/decentralized control. In both scenarios, penetration of 50 MW of WECS is initialized at 15 s; coordinated control is enabled at 30 s; heavy TL5 motor DOL starting at 60 s after FPSO operator signaling at 45 s; unscheduled outage of one SG at 85 s; unscheduled TL6 motor DOL starting at 100 s; and finally a three-phase short-circuit (SC) of 2 s duration on the main feeder is simulated at 118 s, considering a fault impedance of 0.1 Ω.

Figs. 3(a), (b), and (c) show the main feeder RMS pu voltage, PF at the SGs terminals, and the reactive power at the input terminals of the AFE-VFD, respectively. For both strategies, data packets are exchanged between CC and AFE-VFDs within 2 s (i.e., $t_{pbc}$ =2 s). The proposed strategy is tuned with $k$=25 var/V and $f_c$=0.1 Hz, while the literature solution is adjusted according to [10]. WECS penetration at 15 s reduces the PF at terminals of SGs, reducing their efficiency - see Fig. 3(b). Voltage variations at steady-state are caused by power coupling derived from the intermittency of WECS generation, as shown in the zoomed view of Fig. 3(a). Both strategies are enabled at 30 s to regulate PF to $PF^*$ =0.9, coordinating the VFDs to inject reactive power to achieve the desirable $PF^*$. After signaling a planned event at 45 s, the $PF^*$ = 0.9 is changed to 0.8 for both strategies to increase the reactive power availability of VFDs. TL5 DOL motor starting similarly disturbs the FPSO main feeder voltage for both strategies. However, during unplanned SG outage and TL6 DOL motor starting, the proposed strategy enhances voltage support compared to the literature solution - see the zoomed view of Fig. 3(a). For instance, voltage undershoot is improved from 0.83 to 0.91 when adopting the proposed strategy. Among the performed events, the steady-state PF is well regulated around the tuned $PF^*$ in both strategies. Since the centralized control updates every 2 s, PF deviations occur within this period caused by the WECS generation intermittency. The decentralized voltage support smooths the reactive power variation injected by the AFE-VFD - see Fig. 3(c), also improving the steady-state voltage variation at the FPSO main feeder - see Fig. 3(a). For the proposed strategy, a transient voltage improvement regardless of planned or unplanned events and unpredictable disturbances is observed along with PF regulation. Finally, the AFE-VFDs remain controlled for both strategies during 2 s under a three-phase SC that results in low residual voltage of 0.2 pu, which is in accordance with IEEE Std. 1566. The contribution in terms of voltage support is not significant because of the resistive feature of SC and short cabling. However, the proposed method provides more reactive power (i.e., 8.5 Mvar) under the SC duration than method [10] (i.e., 5 Mvar), contributing to reducing the SC current through the SG.

### *B. Effects of parameters variation*

The proposed strategy relies on $k$, $f_c$, and $t_{pbc}$. Several simulations are performed varying these parameters and the

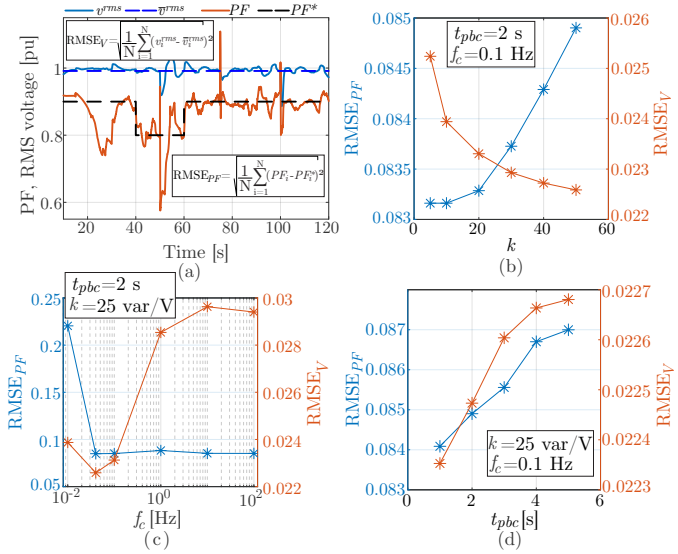


**FIGURE 4. (a) RMSE$_V$ and RMSE$_{PF}$ calculation methodology. RMSE$_V$ and RMSE$_{PF}$ as a function of (b) $k$, (c) $f_c$ and (d) $t_{pbc}$.**

results are shown in Fig. 4. The root mean square error (RMSE) is used to compute the deviation between the expected and measured amounts - see Fig. 4(a). RMSE is a figure of merit that indirectly evaluates the voltage and PF regulation. Lower values of RMSE$_V$ and RMSE$_{PF}$ show more accurate voltage and PF regulation. Figs. 4(b), (c), and (d) show the RMSE for different $k$, $f_c$, and $t_{pbc}$ values, respectively. From Fig. 4(b), higher $k$ value leads to a greater contribution of the decentralized control to $Q_n^*$, worsening the deviation of PF compared to PF$^*$. $k$ =25 var/V shows a good trade-off between RMSE$_V$ and RMSE$_{PF}$, considering fixed $t_{pbc}$ = 2 s and $f_c$ =0.1 Hz. Fig. 4(c) show that low (i.e., <0.04 Hz) and high (> 1 Hz) values of $f_c$ worsen RMSE$_V$ and RMSE$_{PF}$, respectively. If $f_c$ > 1 Hz, the voltage variations caused by intermittent WECS generation and motor starting transients are filtered, degrading the performance of the proposed voltage support strategy. If $f_c$ < 0.04 Hz, the filter response $F$(s) becomes slow, inserting a DC component into $Q_n^{droop}$ and negatively affecting the PF regulation. $f_c$ =0.1 Hz shows a good trade-off between RMSE$_V$ and RMSE$_{PF}$, for fixed $t_{pbc}$ = and $k$ =25 var/V. Finally, Fig. 4(d) shows that increasing $t_{pbc}$ harms both RMSE$_V$ and RMSE$_{PF}$. $f_c$ =0.1 Hz and $k$ =25 var/V are kept constant in Fig. 4(d). The slow update of centralized control results in larger PF deviations and, consequently, larger steps of $Q_n^{centr}$ between the $j$ and ($j$+1)-th control cycle. The $Q_n^{centr}$ deviation disturbs the FPSO voltage, impairing voltage support and raising RMSE$_V$ for higher values of $t_{pbc}$.

## IV. CONCLUSIONS

This paper proposed a centralized control to steer AFE-VFDs to regulate power factor at the terminals of SGs, concomitantly with a decentralized strategy to enhance voltage support under planned/unplanned events and unpredictable disturbances in offshore FPSO units. Simulation results showed that the proposed control is capable of regulating the steady-state power factor on the main feeder, without any knowledge of the FPSO parameters. The proposed strategy suitably provided voltage support under steady-state (i.e., intermittent wind power) and transient-state (i.e., planned/unplanned DOL starting, outage generator, and faults).

## PLAGIARISM POLICY

This article was submitted to the similarity system provided by Crossref and powered by iThenticate – Similarity Check.

## REFERENCES

[1] D. d. S. Mota, E. F. Alves, S. D'Arco, S. Sanchez-Acevedo, E. Tedeschi, "Coordination of Frequency Reserves in an Isolated Industrial Grid Equipped With Energy Storage and Dominated by Constant Power Loads", *IEEE Trans Power Syst*, vol. 39, no. 2, pp. 3271–3285, 2024, doi:10.1109/TPWRS.2023.3304319.

[2] S. Sanchez, E. Tedeschi, J. Silva, M. Jafar, A. Marichalar, "Smart load management of water injection systems in offshore oil and gas platforms integrating wind power", *IET Renew Power Gen*, vol. 11, no. 9, pp. 1153–1162, 2017, doi:https://doi.org/10.1049/iet-rpg.2016.0989.

[3] N. R. Zargari, Z. Cheng, R. Paes, "A Guide to Matching Medium-Voltage Drive Topology to Petrochemical Applications", *IEEE Trans Ind Appl*, vol. 54, no. 2, pp. 1912–1920, 2018, doi:10.1109/PCICON.2017.8188732.

[4] H. M. A. Antunes, D. I. Brandao, V. H. M. Biajo, M. H. S. Alves, F. S. Oliveira, S. M. Silva, "Floating, Production, Storage, and Offloading Unit: A Case Study Using Variable Frequency Drives", *IEEE Trans Ind Appl*, vol. 59, no. 4, pp. 4764–4772, 2023, doi:10.1109/TIA.2023.3258420.

[5] K. d. S. Medeiros, J. M. S. Callegari, L. F. da Rocha, D. I. Brandao, "Power Quality Assessment of Oil and Gas Platform with High Penetration of Floating Offshore Wind Power", *in SPEC/COBEP*, pp. 1–7, 2023, doi:10.1109/SPEC56436.2023.10408371.

[6] F. L. Paes, L. C. Souza, A. M. Dos Santos, L. de Oro Arenas, D. I. Brandao, E. Tedeschi, F. P. Marafão, "Evaluating A Coordinated Control Proposal in Operational Scenarios of an FPSO Oil and Gas Platform", *in 2024 IEEE PCIC Brasil*, pp. 1–8, 2024, doi:10.1109/PCICBrasil54376.2024.10553099.

[7] A. A. Adeyemo, E. Tedeschi, "Technology Suitability Assessment of Battery Energy Storage System for High-Energy Applications on Offshore Oil and Gas Platforms", *Energies*, vol. 16, no. 18, 2023, doi:https://doi.org/10.3390/en16186490.

[8] L. F. da Rocha, D. I. Brandao, K. d. S. Medeiros, M. S. Dall'asta, T. B. Lazzarin, "Coordinated Decentralized Control of Dynamic Volt-Var Function in Oil and Gas Platform With Wind Power Generation", *IEEE Open Journal of Industry Applications*, vol. 4, pp. 269–278, 2023, doi:10.1109/OJIA.2023.3307299.

[9] K. de Sousa Medeiros, L. F. da Rocha, J. M. S. Callegari, D. I. Brandao, "Frequency-Voltage-var Function for VFD in Oil and Gas Platform with Wind Power", *in SPEC/COBEP*, pp. 1–8, 2023, doi:10.1109/SPEC56436.2023.10408441.

[10] J. M. S. Callegari, L. A. Vitoi, D. I. Brandao, "VFD-Based Coordinated Multi-Stage Centralized/Decentralized Control to Support Offshore Electrical Power Systems", *IEEE Trans Smart Grid*, vol. 14, no. 4, pp. 2863–2873, 2023, doi:10.1109/TSG.2022.3224616.

[11] D. I. Brandao, L. S. Araujo, A. M. S. Alonso, G. L. dos Reis, E. V. Liberado, F. P. Marafão, "Coordinated Control of Distributed Three- and Single-Phase Inverters Connected to Three-Phase Three-Wire Microgrids", *IEEE J Emerg Sel Topics Power Electron*, vol. 8, no. 4, pp. 3861–3877, 2020, doi:10.1109/JESTPE.2019.2931122.

[12] M. A. Ahmed, Y. C. Kim, "Hierarchical Communication Network Architectures for Offshore Wind Power Farms", *in IS3C*, pp. 299–303, 2014, doi:10.1109/IS3C.2014.85.